nature physics

LETTERS

PUBLISHED ONLINE: 7 AUGUST 2011 | DOI: 10.1038/NPHYS2055

# Nonlinear phononics as an ultrafast route to lattice control

M. Först[1]*, C. Manzoni[1†], S. Kaiser[1], Y. Tomioka[2], Y. Tokura[3], R. Merlin[4] and A. Cavalleri[1]*

**Two types of coupling between electromagnetic radiation and a crystal lattice have so far been identified experimentally. The first is the direct coupling of light to infrared-active vibrations carrying an electric dipole. The second is indirect, involving electron–phonon coupling and occurring through excitation of the electronic system; stimulated Raman scattering[1–3] is one example. A third path, ionic Raman scattering (IRS; refs 4,5), was proposed 40 years ago. It was posited that excitation of an infrared-active phonon could serve as the intermediate state for Raman scattering, a process that relies on lattice anharmonicities rather than electron–phonon interactions[6]. Here, we report an experimental demonstration of IRS using femtosecond excitation and coherent detection of the lattice response. We show how this mechanism is relevant to ultrafast optical control in solids: a rectified phonon field can exert a directional force onto the crystal, inducing an abrupt displacement of the atoms from their equilibrium positions. IRS opens up a new direction for the optical control of solids in their electronic ground state[7–9], different from carrier excitation[10–14].**

Crystal lattices respond to mid-infrared radiation with oscillatory ionic motions along the eigenvector of the resonantly excited vibration. Let $Q_{IR}$ be the normal coordinate, $P_{IR}$ the conjugate momentum and $\Omega_{IR}$ the frequency of the relevant infrared-active mode, which we assume to be non-degenerate, and $H_{IR} = N(P_{IR}^2 + \Omega_{IR}^2 Q_{IR}^2)/2$ its associated lattice energy ($N$ is the number of cells). For pulses that are short compared with the many-picoseconds decay time of zone-centre optical phonons[15], one can ignore dissipation, and the equation of motion is

$$\ddot{Q}_{IR} + \Omega_{IR}^2 Q_{IR} = \frac{e^* E_0}{\sqrt{M}_{IR}} \sin(\Omega_{IR} t) F(t)$$

where $e^*$ is the effective charge, $M_{IR}$ is the reduced mass of the mode, $E_0$ is the amplitude of the electric field of the pulse and $F$ is the pulse envelope. At times much longer than the pulse width

$$Q_{IR}(t) = \left[\int_{-\infty}^{+\infty} F(\tau)\mathrm{d}\tau\right] \frac{e^* E_0}{\Omega_{IR}\sqrt{M}_{IR}} \cos(\Omega_{IR} t) \qquad (1)$$

For ionic Raman scattering (IRS), the coupling of the infrared-active mode to Raman-active modes is described by the Hamiltonian $H_A = -NAQ_{IR}^2 Q_{RS}$, where $A$ is an anharmonic constant and $Q_{RS}$ is the coordinate of a Raman-active mode, of frequency $\Omega_{RS}$, which is also taken to be non-degenerate. Thus, the equation of motion for the Raman mode is

$$\ddot{Q}_{RS} + \Omega_{RS}^2 Q_{RS} = AQ_{IR}^2 \qquad (2)$$

Ignoring phonon field depletion, it follows from equation (1) that excitation of the infrared mode leads to a constant force on the Raman mode which, for $\Omega_{IR} \gg \Omega_{RS}$, undergoes oscillations of the form

$$Q_{RS}(t) = \frac{A}{2\Omega_{RS}^2}\left[\int_{-\infty}^{+\infty} F(\tau)\mathrm{d}\tau\right]^2 \frac{(e^* E_0)^2}{M_{IR}\Omega_{IR}^2}(1 - \cos\Omega_{RS} t) \qquad (3)$$

around a new equilibrium position. Hence, the coherent nonlinear response of the lattice results in rectification of the infrared vibrational field with the concomitant excitation of a lower-frequency Raman-active mode.

We stress that equation (2) describes a fundamentally different process from conventional stimulated Raman scattering[16–18], for which the driving term $\hat{\Xi}$ in the equation of motion $\ddot{Q}_{RS} + \Omega_{RS}^2 Q_{RS} = \langle\hat{\Xi}\rangle$ depends only on electron variables (see also Supplementary Information).

To date, phonon nonlinearities have been evidenced only by resonantly enhanced second harmonic generation[19,20] or by transient changes in the frequency of coherently excited Raman modes in certain semimetals at high photoexcitation[21]. However, the experimental demonstration of IRS, which offers significant new opportunities for materials control, is still lacking.

Ultrafast optical experiments were performed on single crystal $La_{0.7}Sr_{0.3}MnO_3$, synthesized by the floating zone technique and polished for optical experiments. $La_{0.7}Sr_{0.3}MnO_3$ is a double-exchange ferromagnet with rhombohedrally distorted perovskite structure. Enhanced itinerancy of conducting electrons and relaxation of a Jahn–Teller distortion are observed below the ferromagnetic Curie temperature $T_C = 350$ K (refs 22–24). As a result of the relatively low conductivity, phonon resonances are clearly visible in the infrared spectra at all temperatures[25]. The sample was held at a base temperature of 14 K, in its ferromagnetic phase, and was excited using femtosecond mid-infrared pulses tuned between 9 and 19 μm, at fluences up to 2 mJ cm$^{-2}$. The pulse duration was determined to be 120 fs across the whole spectral range used here. The time-dependent reflectivity was measured using 30-fs pulses at a wavelength of 800 nm.

Figure 1a shows time-resolved reflectivity changes for excitation at 14.3-μm wavelength at 2-mJ cm$^{-2}$ fluence, resonant with the 75-meV (605 cm$^{-1}$) $E_u$ stretching mode[25,26]. The sample reflectivity decreased during the pump pulse, rapidly relaxing into a long-lived state and exhibiting coherent oscillations at 1.2 THz (40 cm$^{-1}$). This frequency corresponds to one of the $E_g$ Raman modes of $La_{0.7}Sr_{0.3}MnO_3$ associated with rotations of the oxygen octahedra[26,27], as sketched in the figure. Consistent with the $E_g$

[1]Max-Planck Research Group for Structural Dynamics, University of Hamburg, Center for Free Electron Laser Science, 22607 Hamburg, Germany, [2]Correlated Electron Engineering Group, AIST, Tsukuba, Ibaraki, 305-8562, Japan, [3]Department of Applied Physics, University of Tokyo, Tokyo, 113-8656, Japan, [4]Department of Physics, University of Michigan, Ann Arbor, Michigan 48109-1040, USA. †Present address: CNR-IFN Dipartimento di Fisica, Politecnico di Milano, 20133 Milan, Italy. *e-mail: michael.foerst@mpsd.cfel.de; andrea.cavalleri@mpsd.cfel.de.

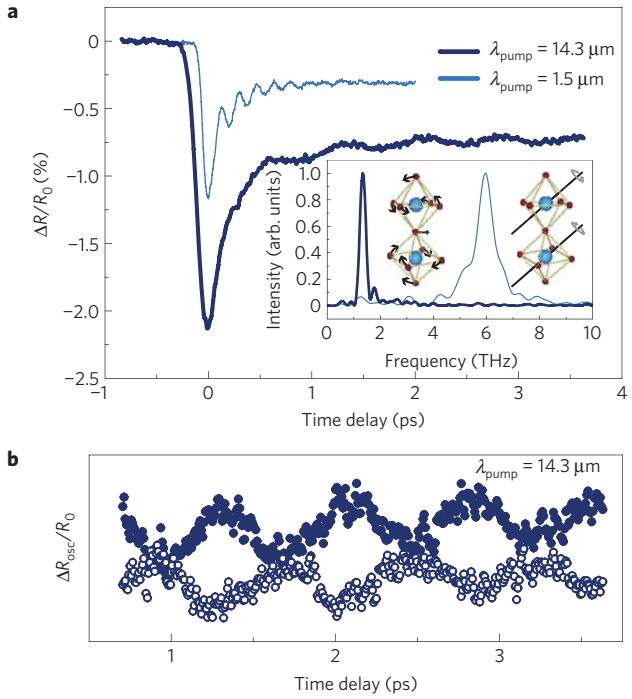


**Figure 1 | Mid-infrared versus near-infrared excitation. a**, Time-resolved reflectivity changes of $La_{0.7}Sr_{0.3}MnO_3$ detected at the central wavelength of 800 nm for mid-infrared excitation at 14.3 μm and near-infrared excitation at 1.5 μm. The inset shows the Fourier transform of the oscillatory signal contributions for different pump wavelengths and the atomic displacements of the corresponding phonon modes. **b**, Signal oscillations for mid-infrared excitation for both parallel (dots) and perpendicular (circles) orientations between the pump and probe polarization. The sample temperature is 14 K.

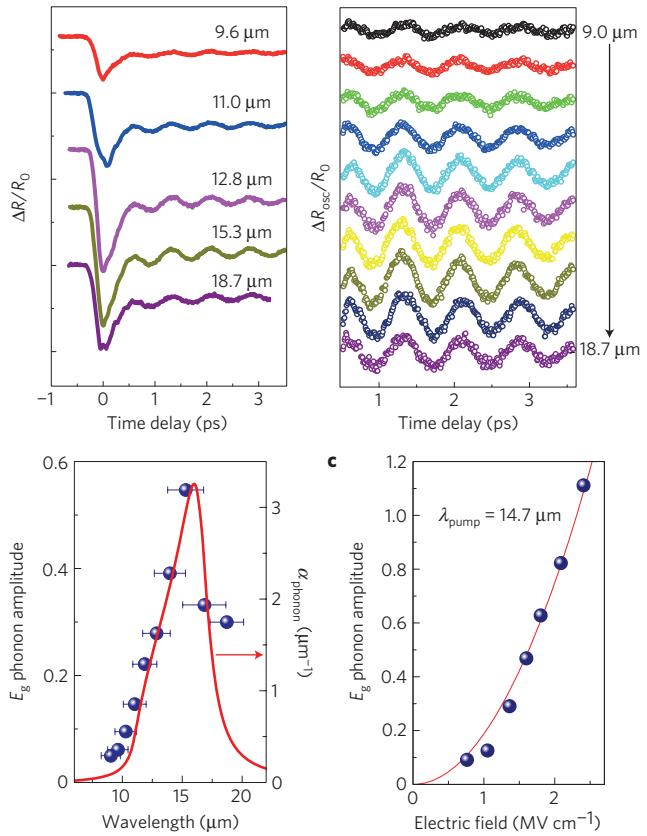


**Figure 2 | Resonant enhancement at the vibrational mode. a**, Differential reflectivity as a function of the central mid-infrared pump wavelength in the vicinity of the frequency of the $MnO_6$ stretching vibration, together with signal oscillations extracted from the data. The pump fluence is 1.1 mJ cm$^{-2}$. **b**, Plot of the coherent $E_g$ phonon amplitude, derived from a fit of the extracted oscillations $\Delta R_{osc}/R_0$ and extrapolation to zero time delay. Results were corrected for wavelength-dependent changes in the reflectivity using data from ref. 25. Horizontal bars are the bandwidths of the mid-infrared pump pulses. The red curve is the linear absorption due to the infrared-active $E_u$ phonon, calculated from the optical data presented in ref. 25. **c**, Dependence of the coherent $E_g$ phonon amplitude on the incident pump electric field measured on resonance at 14.7 μm.

symmetry, we observe a 180° shift of the phase of the oscillations for orthogonal probe polarization (Fig. 1b).

In contrast, excitation in the near-infrared (also shown in Fig. 1a) yielded qualitatively different dynamics. A negative reflectivity change of similar size was observed, comparable to what was observed in the ferromagnetic compound $La_{0.6}Sr_{0.4}MnO_3$ (ref. 28). However, only 5.8-THz oscillations were detected, corresponding to the displacive excitation of the 193-cm$^{-1}$ $A_{1g}$ mode[27,29]. We also measured a comparable response for pump wavelengths all the way down to 575 nm, that is, for excitation from the near-infrared to the visible range only the $A_{1g}$ mode is coherently excited. The $E_g$ mode is observed only for excitation resonant with the $E_u$ phonon mode.

Figure 2(a) shows the time-resolved reflectivity changes for various excitation wavelengths in the mid-infrared spectral range. The panel on the right hand side shows phonon oscillations after Fourier filtering the transient data and subtracting the background. The amplitudes of the initial reflectivity drop of the long-lived state and, as shown in Fig. 2b, the amplitude of the 1.2-THz $E_g$ oscillations show a strong pump-wavelength dependence, with maxima at the phonon resonance. The results in Fig. 2b were obtained from fits to the exponentially damped phonon oscillations, extrapolated to zero time delay; corrections have been made to account for the large wavelength-dependent changes of the reflectivity in the *reststrahlen* band. The amplitude of the $E_g$ oscillations closely follows the spectral shape of the linear absorption of the $E_u$ stretching mode, which we obtained from data reported in ref. 25. Furthermore, as shown in Fig. 2d, we observe a quadratic dependence of the coherent oscillation amplitudes on the incident electric field strength.

These observations are in agreement with the IRS model. According to equation (2), the driving force is second order in the mid-infrared phonon coordinate, and induces a displacive lattice response analogous to rectification through the second-order susceptibility $\chi^{(2)}$ in nonlinear optics. Thus, one expects the IRS response to peak when the infrared pump field is in resonance with the $E_u$ mode, that is, when $Q_{IR}$ is maximum. Second, according to equation (3), a quadratic dependence of the coherent $E_g$ oscillation amplitude on the mid-infrared electric field is expected.

Symmetry considerations also support our interpretation. $La_{0.7}Sr_{0.3}MnO_3$ crystallizes in the distorted perovskite structure of point group $D_{3d}^6$ (space group $R\bar{3}c$). As mentioned above, the representation of the resonantly driven stretching mode is $E_u$, whereas the Raman mode is of $E_g$ symmetry. As $E_g \subset E_u \otimes E_u$, one can write an interaction term of the invariant form

$$H_A = -NA\left[Q_1^{E_g}Q_x^{E_u}Q_y^{E_u} + Q_2^{E_g}\left(Q_x^{E_u}Q_x^{E_u} - Q_y^{E_u}Q_y^{E_u}\right)\right]$$

as required for ionic Raman scattering.

A second experimental observation substantiates our assignment. By using an actively stabilized mid-infrared source based on difference-frequency mixing between two different optical parametric amplifiers[30], we could perform the same experiments with pulses having a stable carrier-envelope phase offset, exciting the

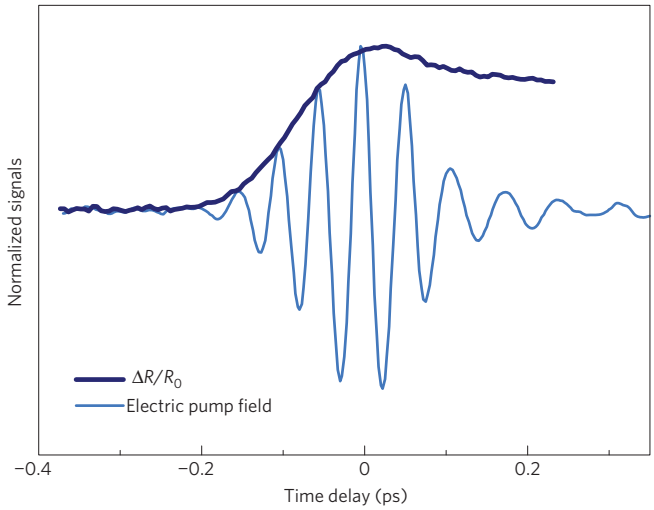


**Figure 3 | Carrier-envelope phase stable excitation.** Relative change of the sample reflectivity induced by carrier-envelope phase stable mid-infrared excitation in resonance with the $E_u$-symmetry stretching vibration (dark blue). The electric field of the pump pulse (light blue), as measured by electro-optic sampling in a 50 μm thick GaSe crystal, is also shown. To increase the temporal resolution, we used as a probe an optical parametric amplifier that delivered broadband infrared pulses (1.2–2.2 μm) compressed to 14 fs. The probe light was spectrally filtered around 1.6 μm in front of the detector.

lattice with a reproducible electric-field phase. Figure 3 shows the time-resolved reflectivity rise alongside the carrier-envelope phase-stable pump field, as measured *in situ* by electro-optic sampling in a 50 μm thick GaSe crystal. The time-dependent reflectivity shows no signature of the absolute electric-field phase, an effect that is well understood for a driving force resulting from rectification of the lattice polarization.

In summary, we have shown that ionic Raman scattering can be used to control crystal structures in a new way, opening the path to selective lattice modifications impossible with electronic excitations. For example, the nonlinear lattice rectification mechanism could be extended to difference-frequency generation between pairs of non-degenerate excitations, leading to new avenues for the control of condensed matter with light beyond linear lattice excitation.

Received 9 January 2011; accepted 25 June 2011; published online 7 August 2011

## References


1. Dhar, L., Rogers, J. A. & Nelson, K. A. Time-resolved vibrational spectroscopy in the impulsive limit. *Chem. Rev.* **94,** 157–193 (1994).
2. Merlin, R. Generating coherent THz phonons with light pulses. *Solid State Commun.* **102,** 207–220 (1997).
3. Dekorsy, T., Cho, G. C. & Kurz, H. in *Light Scattering in Solids VIII* Vol. 76 (eds Cardona, M. & Güntherodt, G.) 169–209 (Topics in Appl. Phys., Springer, 2000).
4. Wallis, R. F. & Maradudin, A. A. Ionic Raman effect II. The first-order ionic Raman effect. *Phys. Rev. B* **3,** 2063–2075 (1971).
5. Martin, T. P. & Genzel, L. Ionic Raman scattering and ionic frequency mixing. *Phys. Status Solide B* **61,** 493–502 (1974).
6. Mills, D. L. Ionic contribution to the Raman tensor of insulators. *Phys. Rev. B* **35,** 9278–9283 (1987).
7. Rini, M. *et al.* Control of the electronic phase of a manganite by mode-selective vibrational excitation. *Nature* **449,** 72–74 (2007).
8. Tobey, R. I., Prabhakaran, D., Boothroyd, A. T. & Cavalleri, A. Ultrafast electronic phase transition in $La_{1/2}Sr_{3/2}MnO_4$ by coherent vibrational excitation: Evidence for non-thermal melting of orbital order. *Phys. Rev. Lett.* **101,** 197404 (2008).
9. Fausti, D. *et al.* Light induced superconductivity in a striped-ordered cuprate. *Science* **331,** 189–191 (2011).
10. Miyano, K., Tanaka, T., Tomioka, Y. & Tokura, Y. Photoinduced insulator-to-metal transition in a perovskite manganite. *Phys. Rev. Lett.* **78,** 4257–4260 (1997).
11. Fiebig, M., Miyano, K., Tomioka, Y. & Tokura, Y. Visualization of the local insulator-metal transition in $Pr_{0.7}Ca_{0.3}MnO_3$. *Science* **280,** 1925–1928 (1998).
12. Cavalleri, A. *et al.* Femtosecond structural dynamics in $VO_2$ during an ultrafast solid–solid phase transition. *Phys. Rev. Lett.* **87,** 237401 (2001).
13. Cavalleri, A., Rini, M. & Schoenlein, R. W. Ultra-broadband femtosecond measurements of the photo-induced phase transition in $VO_2$: From the mid-infrared to the hard X-rays. *J. Phys. Soc. Jpn* **75,** 011004 (2007).
14. Perfetti, L. *et al.* Time evolution of the electronic structure of 1T–$TaS_2$ through the insulator-metal transition. *Phys. Rev. Lett.* **97,** 067402 (2006).
15. Von der Linde, D. & Lambrich, R. Direct measurement of hot-electron relaxation by picosecond spectroscopy. *Phys. Rev. Lett.* **42,** 1090–1093 (1979).
16. Kuznetsov, A. V. & Stanton, C. J. Theory of coherent phonon oscillations in semiconductors. *Phys. Rev. Lett.* **73,** 3243–3246 (1994).
17. Garrett, G. A., Albrecht, T. F., Whitaker, J. F. & Merlin, R. Coherent THz phonons driven by light pulses and the Sb problem: What is the mechanism? *Phys. Rev. Lett.* **77,** 3661–3664 (1996).
18. Stevens, T. E., Kuhl, J. & Merlin, R. Coherent phonon generation and the two stimulated Raman tensors. *Phys. Rev. B* **65,** 144304 (2002).
19. Mayer, A. & Keilmann, F. Far-infrared nonlinear optics. I. $\chi^{(2)}$ near ionic resonance. *Phys. Rev. B* **33,** 6954–6961 (1986).
20. Dekorsy, T., Yakovlev, V. A., Seidel, W., Helm, M. & Keilmann, F. Infrared-phonon–polariton resonance of the nonlinear susceptibility in GaAs. *Phys. Rev. Lett.* **90,** 055508 (2003).
21. Hase, M., Kitajima, M., Nakashima, S-I. & Mizoguchi, K. Dynamics of coherent anharmonic phonons in bismuth using high density photoexcitation. *Phys. Rev. Lett.* **88,** 067401 (2002).
22. Zener, C. Interaction between the *d*-shells in the transition metals. II. Ferromagnetic compounds of manganese with perovskite structure. *Phys. Rev.* **82,** 403–405 (1951).
23. Anderson, P. W. & Hasegawa, H. Considerations on double exchange. *Phys. Rev.* **100,** 675–681 (1955).
24. De Gennes, P. G. Effects of double exchange in magnetic crystals. *Phys. Rev.* **118,** 141–154 (1960).
25. Okimoto, Y., Katsufuji, T., Ishikawa, T., Arima, T. & Tokura, Y. Variation of electronic structure in $La_{1-x}Sr_xMnO_3 (0 = x = 0.3)$ as investigated by optical conductivity spectra. *Phys. Rev. B* **55,** 4206–4214 (1997).
26. Abrashev, M. V. *et al.* Comparative study of optical phonons in the rhombohedrally distorted perovskites $LaAlO_3$ and $LaMnO_3$. *Phys. Rev. B* **59,** 4146–4153 (1999).
27. Granado, E. *et al.* Phonon Raman scattering in $R_{1-x}A_xMnO_{3+\delta}$ (R = La, Pr; A = Ca, Sr). *Phys. Rev. B* **58,** 11435–11440 (1998).
28. Ogasawara, T. *et al.* Photoinduced spin dynamics in $La_{0.6}Sr_{0.4}MnO_3$ observed by time-resolved magneto-optical Kerr spectroscopy. *Phys. Rev. B* **68,** 180407 (2003).
29. Zeiger, H. J. *et al.* Theory for displacive excitation of coherent phonons. *Phys. Rev. B* **45,** 768–778 (1992).
30. Manzoni, C., Först, M., Ehrke, H. & Cavalleri, A. Single-Shot detection and direct control of carrier phase drift of mid-infrared pulses. *Opt. Lett.* **35,** 757–759 (2010).


## Acknowledgements

This work was funded by the Max Planck Society through institutional support for the Max Planck Research Group for Structural Dynamics at the University of Hamburg, and was further supported in part by the US Air Force Office of Scientific Research under contract FA 9550-08-01-0340 through the Multidisciplinary University Research Initiative Program.

## Author contributions

A.C. and M.F. conceived and coordinated the project. M.F. and C.M. developed the experimental apparatus and carried out the experiments. Y. Tomioka and Y. Tokura provided the samples. M.F., C.M., and S.K. analysed the experimental data and interpreted these together with A.C. and R.M.. R.M. developed the analytic theory of Raman scattering. M.F., R.M., and A.C. wrote the manuscript.

## Additional information

The authors declare no competing financial interests. Supplementary information accompanies this paper on www.nature.com/naturephysics. Reprints and permissions information is available online at http://www.nature.com/reprints. Correspondence and requests for materials should be addressed to M.F. or A.C.

nature physics

SUPPLEMENTARY INFORMATION

DOI: 10.1038/NPHYS2055

# Nonlinear phononics as an ultrafast route to lattice control

**Comparison of IRS to conventional Raman excitation.** For excitation of insulators below the gap, and in the absence of phonon absorption, the driving term $\hat{\Xi}$ in the equation of motion $\ddot{Q}_{\mathrm{RS}} + \Omega_{\mathrm{RS}}^2 Q_{\mathrm{RS}} = \left\langle \hat{\Xi} \right\rangle$ depends only on electron variables via

$$\left\langle \Xi \right\rangle \approx \sum_{kl} \frac{\partial \chi_{kl}}{\partial Q_{\mathrm{RS}}} V_{\mathrm{C}} E_k(t) E_l(t) .$$

Here $\partial \chi_{kl} / \partial Q_{\mathrm{RS}}$ is the Raman tensor and $V_{\mathrm{C}}$ is the cell volume. For a fully symmetric mode, the corresponding equation of motion is

$$\ddot{Q}_{\mathrm{RS}} + \Omega_{\mathrm{RS}}^2 Q_{\mathrm{RS}} = \left( \partial \chi / \partial Q_{\mathrm{RS}} \right) V_{\mathrm{C}} \left[ E_0 \sin(\omega_{\mathrm{L}} t) F(t) \right]^2$$

with $\omega_{\mathrm{L}}$ (>> $\Omega_{\mathrm{RS}}$) the laser carrier-frequency. For $t \to \infty$

$$Q_{\mathrm{RS}}(t) = \left[ \int_{-\infty}^{+\infty} F^2(\tau) d\tau \right] \frac{V_{\mathrm{C}} E_0^2}{2\Omega_{\mathrm{RS}}} \frac{\partial \chi}{\partial Q_{\mathrm{RS}}} \sin(\Omega_{\mathrm{RS}} t) .$$

Thus, the ratio between ionic, $\sigma_{\mathrm{I}}$, and electronic-mediated Raman scattering cross section, $\sigma_{\mathrm{E}}$ can be estimated as

$$\sigma_{\mathrm{I}} / \sigma_{\mathrm{E}} \sim \frac{e^{*2}}{M_{\mathrm{IR}} \Omega_{\mathrm{RS}}^2 V_{\mathrm{C}}} \frac{\gamma_{\mathrm{G}}}{\partial \chi / \partial V_{\mathrm{C}}} ,$$

where $\gamma_{\mathrm{G}} = \partial \ln \Omega_{\mathrm{RS}} / \partial V_{\mathrm{C}}$ is the Grüneisen parameter. Since $\gamma_{\mathrm{G}} \sim \partial \chi / \partial V_{\mathrm{C}} \sim V_{\mathrm{C}}^{-1}$, the two cross sections are of similar magnitude.